1150 *Organometallics* **2010,** *29,* 1150–1156
DOI: 10.1021/om901025q

ORGANOMETALLICS
Article

Bimetallic Ruthenium Complexes: Synthesis, Characterization, and the Effect of Appending Long Carbon Chains to Their Bridges

Xiang-Hua Wu, Jin Hua Liang, Jian-Long Xia, Shan Jin, Guang-Ao Yu, and Sheng Hua Liu*

Key Laboratory of Pesticide and Chemical Biology, Ministry of Education, College of Chemistry, Central China Normal University, Wuhan 430079, People's Republic of China

Received November 26, 2009

A series of binuclear ruthenium complexes $[RuCl(CO)(PMe_3)_3]_2(\mu\text{-CH}{=}\text{CH}{-}\text{Ar}{-}\text{CH}{=}\text{CH})$ (Ar = $C_6H_2(OR)_2$-2,5; R = CH_3 (**4a**), $^nC_4H_9$ (**4b**), $^nC_6H_{13}$ (**4c**), $^nC_8H_{17}$ (**4d**), $^nC_{10}H_{21}$ (**4e**), $^nC_{12}H_{25}$ (**4f**), $^nC_{14}H_{29}$ (**4g**)), $[RuCl(CO)(PMe_3)_3]_2(\mu\text{-CH}{=}\text{CH}{-}\text{Ar}{-}{\equiv}{-}\text{Ar}{-}\text{CH}{=}\text{CH})$ (Ar = $C_6H_2(R)_2$-2,5; R = OCH_3 (**10a**), $O^nC_8H_{17}$ (**10b**), H (**10c**)), and $[RuCl(CO)(PMe_3)_3]_2(\mu\text{-CH}{=}\text{CH}{-}\text{Ar}{-}{\equiv}{-}\text{Ar}{-}{\equiv}{-}\text{Ar}{-}\text{CH}{=}\text{CH})$ (Ar = $C_6H_2(R)_2$-2,5; R = OCH_3 (**13a**), $O^nC_8H_{17}$ (**13b**), H (**13c**)) have been synthesized. These complexes have been characterized by elemental analysis, NMR, and UV/vis spectrophotometry. The structures of **4b** and **4d** have been determined by X-ray crystallography. Electrochemical studies have shown that long carbon chains attached to the bridges of the complexes facilitate the stability of mixed-valence bimetallic ruthenium complexes.

Introduction

Linear conjugated organometallic complexes in which two redox-active transition metal moieties are connected by molecule-based wires have been extensively investigated.[1−5] Understanding of charge-transfer processes at the nanoscale level has attracted intense interest recently.[6] However, electronic coupling between two electroactive groups decays dramatically with increasing length of the bridging ligands, as in $[(\eta^5\text{-}C_5Me_5)Re(NO)(PPh_3)_2(C{\equiv}C)_n]$ ($n = 2, \Delta E = 0.53$ V; $n = 3, \Delta E = 0.38$ V; $n = 4, \Delta E = 0.28$ V; $n = 5, \Delta E = 0.20$ V; $n = 6, \Delta E = 0.19$ V; $n = 8, \Delta E = 0.09$ V; $n = 10, \Delta E < 0.07$ V).[7] The wave separation or potential difference ($\Delta E_{1/2}$) is representative of the thermodynamic stability of the corresponding mixed-valence metal species and is a critical measure to evaluate electronic delocalization along the conjugated molecular backbones in mixed-valence metal species.[1e] The question then arises as to how this attenuation might be

*Corresponding author. E-mail: chshliu@mail.ccnu.edu.cn.

(1) (a) Casey, C. P.; Audett, J. D. *Chem. Rev.* **1986**, *86*, 339. (b) Schwab, P. F. H.; Levin, M. D.; Michl, J. *Chem. Rev.* **1999**, *99*, 1863. (c) Holton, J.; Lappert, M. F.; Pearce, R.; Yarrow, P. I. *Chem. Rev.* **1983**, *83*, 135. (d) Moss, J. R.; Scott, L. G. *Cood. Chem. Rev.* **1984**, *60*, 171. (e) Paul, F.; Lapinte, C. *Coord. Chem. Rev.* **1998**, *178−180*, 431. (f) Ren, T. *Chem. Rev.* **2008**, *108*, 4185.

(2) (a) Bartik, T.; Bartik, B.; Brady, M.; Dembinski, R.; Gladysz, J. A. *Angew. Chem., Int. Ed. Engl.* **1996**, *35*, 414–417. (b) Zheng, Q.; Gladysz, J. A. *J. Am. Chem. Soc.* **2005**, *127*, 10508. (c) Zheng, Q.; Bohling, J. C.; Peters, T. B.; Frisch, A. C.; Hampel, F.; Gladysz, J. A. *Chem.—Eur. J.* **2006**, *12*, 6486. (d) Stahl, J.; Mohr, W.; de Quadras, L.; Peters, T. B.; Bohling, J. C.; Martín-Alvarez, J. M.; Owen, G. R.; Hampel, F.; Gladysz, J. A. *J. Am. Chem. Soc.* **2007**, *129*, 8282. (e) Owen, G. R.; Stahl, J.; Hampel, F.; Gladysz, J. A. *Chem.—Eur. J.* **2008**, *14*, 73.

(3) (a) Ren, T.; Zou, G.; Alvarez, J. C. *Chem. Commun.* **2000**, 1197. (b) Xu, G. L.; Ren, T. *Organometallics* **2001**, *20*, 2400. (c) Ren, T.; Xu, G. L. *Comments Inorg. Chem.* **2002**, *23*, 355. (d) Ren, T.; Xu, G. L. *Comments on Inorg. Chem.* **2002**, *23*, 355. (e) Xu, G.-L.; Zou, G.; Ni, Y.-H.; DeRosa, M. C.; Crutchley, R. J.; Ren, T. *J. Am. Chem. Soc.* **2003**, *125*, 10057. (f) Shi, Y. H.; Yee, G. T.; Wang, G. B.; Ren, T. *J. Am. Chem. Soc.* **2004**, *126*, 10552. (g) Blum, A. S.; Ren, T.; Parish, D. A.; Trammell, S. A.; Moore, M. H.; Kushmerick, J. G.; Xu, G.-L.; Deschamps, J. R.; Pollack, S. K.; Shashidhar, R. *J. Am. Chem. Soc.* **2005**, *127*, 10010. (h) Ren, T. *Organometallics* **2005**, *24*, 4854.

(4) (a) Paul, F.; da Costa, G.; Bondon, A.; Gauthier, N.; Sinbandhit, S.; Toupet, L.; Costuas, T.; Halet, J. -F.; Lapinte, C. *Organometallics* **2007**, *26*, 874. (b) Paul, F.; Ellis, B. G.; Bruce, M. I.; Toupet, L.; Costuas, T.; Halet, J.-F.; Lapinte, C. *Organometallics* **2006**, *25*, 649. (c) Paul, F.; Toupet, L.; Thepot, J.-Y.; Costuas, K.; Halet, J.-F.; Lapinte, C. *Organometallics* **2005**, *24*, 5464. (d) Costuas, K.; Paul, F.; Toupet, L.; Halet, J.-F.; Lapinte, C. *Organometallics* **2004**, *23*, 2053. (e) Paul, F.; Costuas, K.; Ledoux, I.; Deveau, S.; Zyss, J.; Halet, J.-F.; Lapinte, C. *Organometallics* **2002**, *21*, 5229. (f) Denis, R.; Toupet, L.; Paul, F.; Lapinte, C. *Organometallics* **2000**, *19*, 4240. (g) Bruce, M. I.; Low, P. J.; Costuas, K.; Halet, J.-F.; Best, S. P.; Heath, G. A. *J. Am. Chem. Soc.* **2000**, *122*, 1949. (h) Bruce, M. I.; Cole, M.; Gaudio, M.; Skelton, B. W.; White, A. H. *J. Organomet. Chem.* **2006**, *691*, 4601. (i) Antonova, A. B.; Bruce, M. I.; Humphrey, P. A.; Gaudio, M.; Nicholson, B. K.; Scoleri, N.; Skelton, B. W.; White, A. H.; Zaitseva, N. N. *J. Organomet. Chem.* **2006**, *691*, 4696. (j) Bruce, M. I.; Ellis, B. G.; Low, P. J.; Skelton, B. W.; White, A. H. *Organometallics* **2003**, *22*, 3184. (k) Bruce, M. I.; Costuas, K.; Davin, T.; Ellis, B. G.; Halet, J.-F.; Lapinte, C.; Low, P. J.; Smith, M. E.; Skelton, B. W.; Toupet, L.; White, A. H. *Organometallics* **2005**, *24*, 3684. (l) Bruce, M. I.; Low, P. J.; Hartl, F.; Humphrey, P. A.; Montigny, F. D.; Jevric, M.; Lapinte, C.; Perkins, G. J.; Roberts, R. L.; Skelton, B. W.; White, A. H. *Organometallics* **2005**, *24*, 5241.

(5) (a) Gao, L.-B.; Zhang, L.-Y.; Shi, L.-X.; Chen, Z.-N. *Organometallics* **2005**, *24*, 1678. (b) Gao, L.-B.; Liu, S.-H.; Zhang, L.-Y.; Shi, L.-X.; Chen, Z.-N. *Organometallics* **2006**, *25*, 506. (c) Gao, L.-B.; Kan, J.; Fan, Y.; Zhang, L.-Y.; Liu, S.-H.; Chen, Z.-N. *Inorg. Chem.* **2007**, *46*, 5651. (d) Yuan, P.; Wu, X. H.; Yu, G.; Du, D.; Liu, S. H. *J. Organomet. Chem.* **2007**, *692*, 3588. (e) Wu, X. H.; Jin, S.; Liang, J. H.; Li, Z. Y.; Yu, G.; Liu, S. H. *Organometallics* **2009**, *28*, 2450. (f) Liu, S. H.; Hu, Q. Y.; Xue, P.; Wen, T. B.; Williams, I. D.; Jia, G. *Organometallics* **2005**, *24*, 769. (g) Hu, Q. Y.; Lu, W. X.; Tang, H. D.; Sung, H. H. Y.; Wen, T. B.; Williams, I. D.; Wong, G. K. L.; Lin, Z.; Jia, G. *Organometallics* **2005**, *24*, 3966. (h) Liu, S. H.; Xia, H.; Wen, T. B.; Zhou, Z. Y.; Jia, G. *Organometallics* **2003**, *22*, 737. (i) Liu, S. H.; Chen, Y.; Wan, K. L.; Wen, T. B.; Zhou, Z.; Lo, M. F.; Williams, I. D.; Jia, G. *Organometallics* **2002**, *21*, 4984. (j) Xia, H. P.; Ng, W. S.; Ye, J. S.; Li, X. Y.; Wong, W. T.; Lin, Z.; Yang, C.; Jia, G. *Organometallics* **1999**, *18*, 4552. (k) Xia, H. P.; Wu, W. F.; Ng, W. S.; Williams, I. D.; Jia, G. *Organometallics* **1997**, *16*, 2940. (l) Xia, J.-L; Wu, X.; Lu, Y.; Chen, G.; Jin, S.; Yu, G.; Liu, S. H. *Organometallics* **2009**, *28*, 2701.

 Published on Web 02/10/2010

Scheme 1

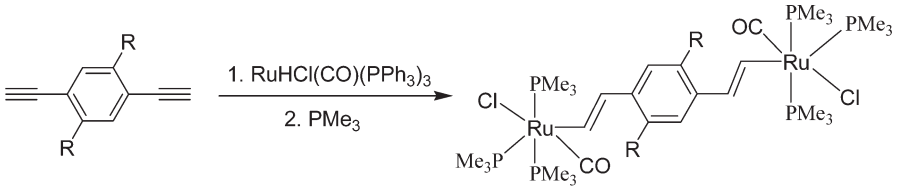

R = OCH_3 **3a**
R = $O^nC_4H_9$ **3b**
R = $O^nC_6H_{13}$ **3c**
R = $O^nC_8H_{17}$ **3d**
R = $O^nC_{10}H_{21}$ **3e**
R = $O^nC_{12}H_{25}$ **3f**
R = $O^nC_{14}H_{29}$ **3g**

R = OCH_3 **4a**
R = $O^nC_4H_9$ **4b**
R = $O^nC_6H_{13}$ **4c**
R = $O^nC_8H_{17}$ **4d**
R = $O^nC_{10}H_{21}$ **4e**
R = $O^nC_{12}H_{25}$ **4f**
R = $O^nC_{14}H_{29}$ **4g**

Scheme 2

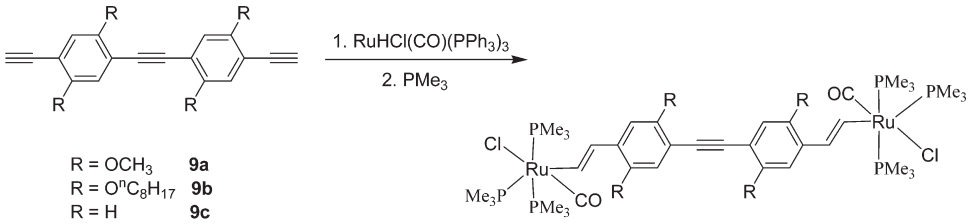

R = OCH_3 **9a**
R = $O^nC_8H_{17}$ **9b**
R = H **9c**

R = OCH_3 **10a**
R = $O^nC_8H_{17}$ **10b**
R = H **10c**

prevented. In this context, some research groups have recently reported that intermetallic electronic communication between the two ferrocene centers could be enhanced by incorporating metal moieties such as $[Ru(dppm)_2]$[8] or $[Pt_2(dppm)]$,[9] and more especially $[Ru_2(DMBA)_4]$,[10] where DMBA is *N,N′*-dimethylbenzamidinate. This suggests that some conjugated complexes incorporating metal moieties may act as better electronic conductors than their all-carbon analogues.

Previously, we reported that electronic coupling between two Ru centers could be fine-tuned by modification of a 1,4-diethenylphenylene bridging ligand and that the attachment of an electron-releasing substituent (such as OCH_3) facilitated electron coupling.[5e] Pelter et al. reported that two OR groups on a benzene unit greatly enhanced the solubility of such oligomers as well as their electronic effects.[11] To probe the efficiency of charge transfer across the molecular fragment −Ar−, electron-releasing OR substituents with alkyl chains of different lengths have been introduced. To understand the electronic effects of these substituents at the nanoscale level with a view to limiting the attenuation of electronic coupling between two Ru centers with increasing length of the molecular wire, some oligomeric binuclear complexes have been prepared. The electrochemical properties of these binuclear complexes have been investigated by voltammetric techniques.

Results and Discussion

Syntheses and Characterization. Substituted 1,4-diethynylbenzene derivatives **3a**−**g** were synthesized by a sequence of coupling and deprotection reactions according to methods reported in the literature. Compound **9a** was obtained by multiple Sonogashira couplings and selective deprotections (Supporting Information). The starting reagent 1,4-diiodo-2,5-dimethoxybenzene (**1a**)[12] was subjected to monoiodo coupling with 2-methyl-3-butyn-2-ol to afford **5a**.[13] The remaining iodo substituent in **5a** was subsequently coupled with trimethylsilylethyne, also under Sonogashira conditions, to give **6a**. Selective deprotection of the trimethylsilyl protecting group with K_2CO_3 in $MeOH/CH_2Cl_2$ gave the corresponding terminal alkyne **7a**. Compound **7a** was then coupled with the previously prepared iodide **5a** to afford **8a**.

(6) (a) Adams, D. M.; Brus, L.; Chidsey, C. E. D.; Creager, S.; Creutz, C.; Kagan, C. R.; Kamat, P. V.; Lieberman, M.; Lindsay, S.; Marcus, R. A.; Metzger, R. M.; Michel-Beyerle, M. E.; Miller, J. R.; Newton, M. D.; Rolison, D. R.; Sankey, O.; Schanze, K. S.; Yardley, J.; Zhu, X. Y. *J. Phys. Chem. B* **2003**, *107*, 6668. (b) Barbara, P. F.; Meyer, T. J.; Ratner, M. A. *J. Phys. Chem.* **1996**, *100*, 13148. (c) Nitzan, A.; Ratner, M. A. *Science* **2003**, *300*, 1384.

(7) (a) Horn, C. R.; Martin-Alvarez, J. M.; Gladysz, J. A. *Organometallics* **2002**, *21*, 5386. (b) Horn, C. R.; Gladysz, J. A. *J. Eur. Inorg. Chem.* **2003**, 2211. (c) Dembinski, R.; Bartik, T.; Bartik, B.; Jaeger, M.; Gladysz, J. A. *J. Am. Chem. Soc.* **2000**, *122*, 810. (d) Brady, M.; Weng, W.; Zhou, Y.; Seyler, J. W.; Amoroso, A. J.; Arif, A. M.; Böhme, M.; Frenking, G.; Gladysz, J. A. *J. Am. Chem. Soc.* **1997**, *119*, 775.

(8) (a) Levanda, C.; Bechgaard, K.; Cowan, D. O. *J. Org. Chem.* **1976**, *41*, 2700. (b) Zhu, Y.; Clot, O.; Wolf, M. O.; Yap, G. P. *J. Am. Chem. Soc.* **1998**, *120*, 1812. (c) Jones, N. D.; Wolf, M. O.; Giaquinta, D. M. *Organometallics* **1997**, *16*, 1352.

(9) Yip, J. H. K.; Wu, J.; Wong, K.-Y.; Ho, K. P.; Pun, C. S.-N.; Vittal, J. J. *Organometallics* **2002**, *21*, 5292.

(10) (a) Xu, G. L.; DeRosa, M. C.; Crutchley, R. J.; Ren, T. *J. Am. Chem. Soc.* **2004**, *126*, 3728. (b) Xu, G. L.; Crutchley, R. J.; DeRosa, M. C.; Pan, Q. J.; Zhang, H. X.; Wang, X. P.; Ren, T. *J. Am. Chem. Soc.* **2005**, *127*, 13354. (c) Xi, B.; Xu, G.-L.; Fanwick, P. E.; Ren, T. *Organometallics* **2009**, *28*, 2338.

(11) Pelter, A.; Jones, D. E. *J. Chem. Soc., Perkin Trans. 1* **2000**, 2289.

(12) Waybright, S. M.; Singleton, C. P.; Wachter, K.; Murphy, C. J.; Bunz, U. H. F. *J. Am. Chem. Soc.* **2001**, *123*, 1828.

(13) Sasaki, T.; Tour, J. M. *Tetrahedron Lett.* **2007**, *48*, 5821.

Scheme 3

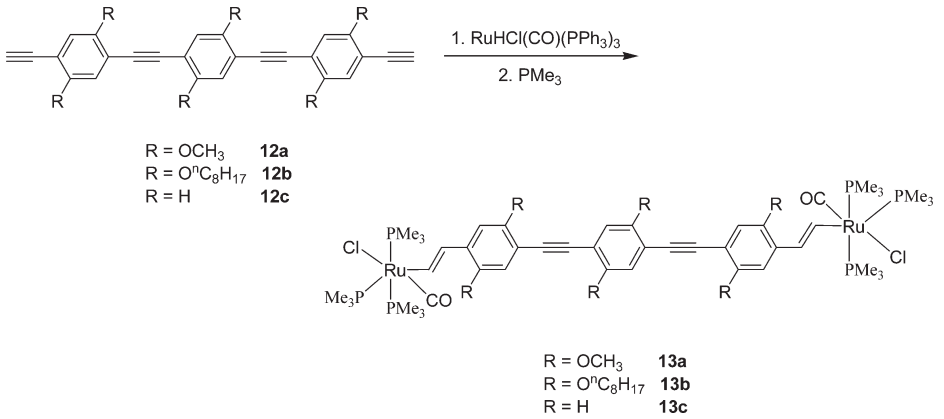

Table 1. Crystal Data, Data Collection, and Refinement Parameters for 4b and 4d

	4b	4d
formula	$C_{38}H_{78}Cl_2O_4P_6Ru_2$	$C_{46}H_{94}Cl_2O_4P_6Ru_2$
fw	1057.86	1170.07
temp (K)	299(2)	200(2)
cryst syst	tetragonal	tetragonal
space group	$P4_2/n$	$P4_2/n$
a (Å)	25.6226(7)	25.1492(7)
b (Å)	25.6226(7)	25.1492(7)
c (Å)	9.6058(5)	9.6436(6)
β (deg)	90.00	90.00
V (Å^{-3})	6306.4(4)	6099.4(4)
Z	4	4
D_{calcd} (g cm^{-3})	1.114	1.274
a, b for W^a	0.0911, 0.0000	0.0742, 5.4310
final R	0.0715	0.0514
R_w	0.1640	0.1355
R (all data)	0.1199	0.0614
R_w (all data)	0.1806	0.1435
goodness of fit/F^2	1.003	0.110

^{a} $W = 1/[\sigma^2(F_o)^2 + (aP)^2 + bP]$, where $P = (F_o^2 + F_c^2)/3$.

Table 2. Selected Bond Lengths (Å) and Angles (deg) for 4b and 4d

	4b	4d
C(11)−C(12)	1.317(8)	1.333(5)
C(12)−C(13)	1.478(8)	1.478(5)
C(13)−C(14)	1.404(8)	1.393(5)
C(13)−C(15)	1.373(9)	1.414(5)
C(14)-O(1′)	1.395(9)	
C(16′)-O(1′)	1.372(10)	
C(15)−O(2)		1.385(4)
O(2)−C(16)		1.394(6)
C(10)−Ru(1)	1.801(9)	1.824(4)
C(11)−Ru(1)	2.105(5)	2.102(3)
C(12)−C(11)−Ru(1)	179.2(8)	132.3(3)
C(11)−C(12)−C(13)	128.5(7)	126.6(3)
C(12)−C(13)−C(14)	121.3(6)	123.6(3)
C(13)−C(14)−O(1′)	112.9(9)	
C(13)−C(15)−O(2)		119.2(3)
C(10)−Ru(1)−C(11)	90.3(3)	90.51(15)
C(11)−Ru(1)−Cl(1)		87.36(11)
C(11)−Ru(1)−Cl(2)	87.58(17)	

The 2-hydroxy-2-propyl fragments were removed by refluxing **8a** in toluene in the presence of sodium hydroxide to give the corresponding diterminal alkyne **9a**. Following the above procedures, compounds **5b**−**9b** were prepared analogously. Twofold Sonogashira reaction of **5a** with the diterminal alkyne **3a** gave **11a**. Treatment of the latter compound with NaOH in toluene afforded the diterminal alkyne **12a** (Supporting Information). Likewise, compounds **11b** and 12b were obtained under the same conditions.

Reactions of the diethynylaryls **3a**−**g**, **9a**−**c**, and **12a**−**c** with the ruthenium hydride complex $[RuHCl(CO)(PPh_3)_3]$ afforded the corresponding insertion products $[(PPh_3)_2Cl(CO)Ru]_2(\mu\text{-CH=CH-Ar-CH=CH})$, $[(PPh_3)_2Cl(CO)Ru]_2(\mu\text{-CH=CH-Ar-}\equiv\text{-Ar-CH=CH})$, and $[(PPh_3)_2Cl(CO)Ru]_2(\mu\text{-CH=CH-Ar-}\equiv\text{-Ar-}\equiv\text{-Ar-CH=CH})$, respectively, which were not isolated because they are air-sensitive, especially in solution. PMe_3 was then added to give the corresponding six-coordinated complexes **4a**−**g**, **10a**−**c**, and **13a**−**c**, respectively (Schemes 1, 2, and 3). These complexes were characterized by NMR. The PMe_3 ligands in all of these bimetallic complexes are meridionally coordinated to ruthenium, as indicated by an AM_2 pattern in the $^{31}P\{^1H\}$ NMR spectra.

X-ray Structures of 4b and 4d. The molecular structures of **4b** and **4d** were determined by X-ray crystallography. The crystallographic details are given in Table 1. Selected bond distances and angles for **4b** and **4d** are presented in Table 2. The molecular structures of **4b** and **4d** are depicted in Figures 1 and 2, respectively. The rod-like binuclear ruthenium arrays in **4b** and **4d** consist of two $[(PMe_3)_3Cl(CO)Ru]$ end-groups linked by a μ-CH=CH−Ar−CH=CH (Ar = $C_6H_2(OC_4H_9)_2$-2,5 (**4b**), $C_6H_2(OC_8H_{17})_2$-2,5 (**4d**)) carbon chain through Ru−C σ-bonding. The molecular structures of **4b** and **4d** are centrosymmetric, and some C atoms in the OR groups are disordered. The two Ru centers are related by a pseudo-C_2 rotation axis. The distances of two Ru atoms in complexes **4b** and **4d** are 11.913 and 11.906 Å, respectively, both of which are shorter than that of 11.919 Å in complex **4a**.[5e] The carbon atoms of the two CH=CH units and benzene ring are nearly coplanar, with dihedral angles between the core benzene ring and the two vinyl groups of 4.63° in **4b** and 6.10° in **4d**, respectively. The overall geometry about the two ruthenium centers in **4b** and **4d** closely resembles that in the bimetallic ruthenium complexes $[RuCl(CO)(PMe_3)_3]_2(\mu\text{-(CH=CH)}_n)$[5f,h,i] and $[RuCl(CO)(PMe_3)_3]_2(\mu\text{-CH=CH-C}_6H_2(R)_2\text{-2,5-CH=CH})$ (R = CH_3, OCH_3).[5e] The two complexes adopt the same crystal system and space group, as can be seen in Table 1, which are distinct from those of complex **4a**.

Electronic Absorption Spectroscopy. The electronic properties of the present bimetallic complexes were investigated by optical absorption spectroscopy. For complexes **4b**−**g**, but not for **4a**, a rather intense electronic transition is seen at around 349 nm (Table 3), which can be attributed to $\pi-\pi^*$

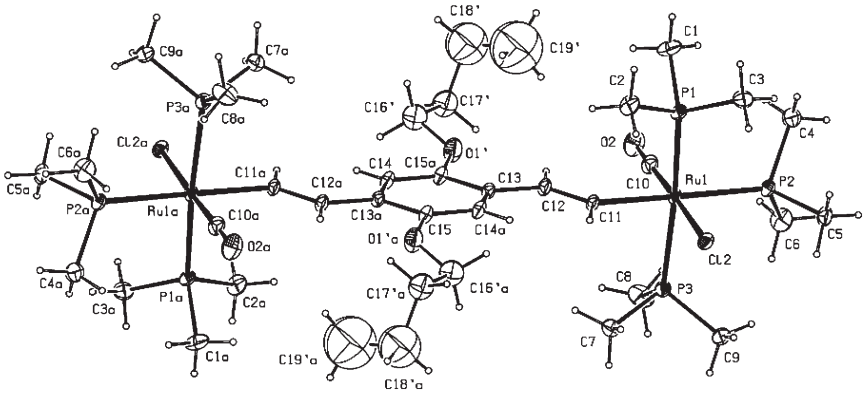

Figure 1. Molecular structure of **4b**.

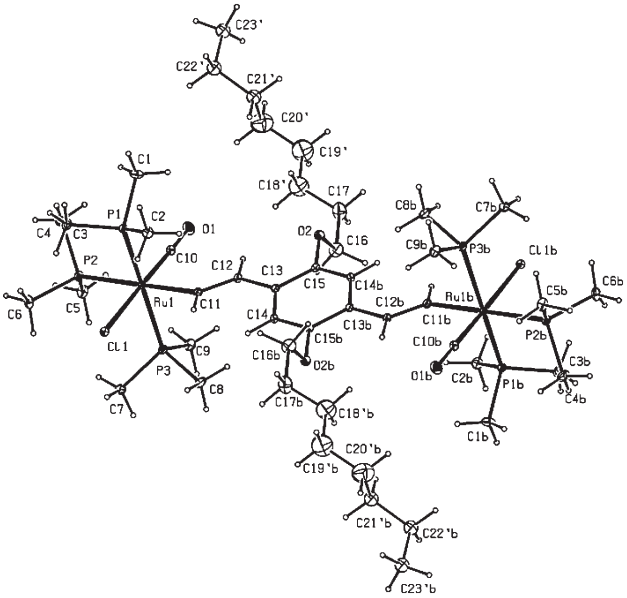

Figure 2. Molecular structure of **4d**.

Table 3. UV−Vis Data for Binuclear Complexes 4a−g, 10a−c, and 13a−c in CH_2Cl_2

complex	abs, nm ($10^{-4}\varepsilon$, M^{-1} cm^{-1})
4a	357 (1.15)[5e]
4b	350 (16.4)
4c	349 (16.5)
4d	349 (16.5)
4e	350 (16.3)
4f	349 (18.1)
4g	349 (18.1)
10a	372 (2.0)
10b	388 (5.6)
10c	415 (6.4)
13a	376 (2.3)
13b	394 (4.7)
13c	418 (8.4)

ligand-centered transitions. Compared with the absorption spectrum of the unsubstituted complex **10c**, the absorption maxima of the substituted complexes **10a** and **10b** show bathochromic shifts and the intensities of the bands are increased. The above results are supported by comparison of the absorption spectra of complexes **13a−c**. A red-shift and an increase in intensity are observed upon extension of the π-system of the bridging spacer.

Table 4. Electrochemical Data for Complexes 4a−g in CH_2Cl_2

complex	$E_{1/2}$(A)	$E_{1/2}$(B)	$\Delta E_{1/2}$[a]	K_c[b]
4a	0.10	0.46	0.35	8.2×10^5
4b	0.07	0.44	0.37	1.8×10^6
4c	0.07	0.44	0.37	1.8×10^6
4d	0.08	0.45	0.37	1.8×10^6
4e	0.10	0.47	0.37	1.8×10^6
4f	0.12	0.49	0.37	1.8×10^6
4g	0.11	0.48	0.37	1.8×10^6

[a] $\Delta E_{1/2} = E_{1/2}(B) - E_{1/2}(A)$ denotes the potential difference between redox processes A and B. [b] The comproportionation constants, K_c, were calculated by the formula $K_c = \exp(\Delta E_{1/2}/25.69)$ at 298 K.[14]

Electrochemistry. The redox behavior of the present bimetallic complexes (1 mM in CH_2Cl_2 or THF) was investigated by cyclic voltammetry and square-wave voltammetry techniques with 0.1 M nBu$_4$NPF$_6$ as the supporting electrolyte. Complexes **4b−g** in CH_2Cl_2 undergo two successive one-electron oxidation processes, giving rise to redox waves A and B (Table 4) in the potential region 0.06−0.50 V (Figure S1), corresponding to oxidation of $Ru_2^{II,II}$ to $Ru_2^{II,III}$ and then of $Ru_2^{II,III}$ to $Ru_2^{III,III}$. As shown in Table 4, for complex **4b**, with two OC_4H_9 groups attached to the 1,4-diethenylphenylene spacer unit, the $\Delta E_{1/2}$ is 0.37 V, with the corresponding K_c being 1.8×10^6. Compared with the $\Delta E_{1/2}$ (0.35 V) and K_c value (8.2×10^5) of complex **4a**, the OC_4H_9 group is apparently even more favorable for the stability of the mixed-valence complex than the OCH_3 group. However, by comparison of the $\Delta E_{1/2}$ and K_c values of complexes **4c−g** (Table 4), it is found that the stability of the mixed-valence complex is not enhanced further with a further increase of n to give longer OC_nH_{2n+1} moieties.

Complex **10c** in CH_2Cl_2 undergoes two one-electron irreversible processes, with ΔE_p being 0.08 V and the corresponding K_c being 22.5 (Table 5). Compared to the voltammetric features of the complex $[RuCl(CO)(PMe_3)_3]_2$-(μ-CH=CH−C_6H_4−CH=CH), for which the $\Delta E_{1/2}$ value is 0.29 V and the K_c value is 8.0×10^4,[5e] it is clear that the stability of the mixed-valence complex is rapidly attenuated on increasing the length of the bridging ligand. However, if OCH_3 groups are introduced on the −Ar− unit, as in complex **10a**, both the oxidation and reduction couples are cathodically shifted and the stability of the mixed-valence complex is slightly increased ($\Delta E_{1/2}$ = 0.09 V), which may be attributed to the electron-donating property of the OCH_3 group. On going to the OC_8H_{17}-bearing structure **10b**, which displays two resolved one-electron redox couples for the two Ru centers, the separation of redox couples increases further

Table 5. Electrochemical Data for Complexes 10a−c in CH_2Cl_2

complex	$E_{1/2}$(A)	$E_{1/2}$(B)	$\Delta E_{1/2}$[a]	K_c[b]
10a	0.36	0.45	0.09	33.2
10b	0.34	0.46	0.12	1.1×10^2
10c	0.58	0.66	0.08[c]	22.5

[a] $\Delta E_{1/2} = E_{1/2}(B) - E_{1/2}(A)$ denotes the potential difference between redox processes A and B. [b] The comproportionation constants, K_c, were calculated by the formula $K_c = \exp(\Delta E_{1/2}/25.69)$ at 298 K.[14] [c] ΔE_p value.

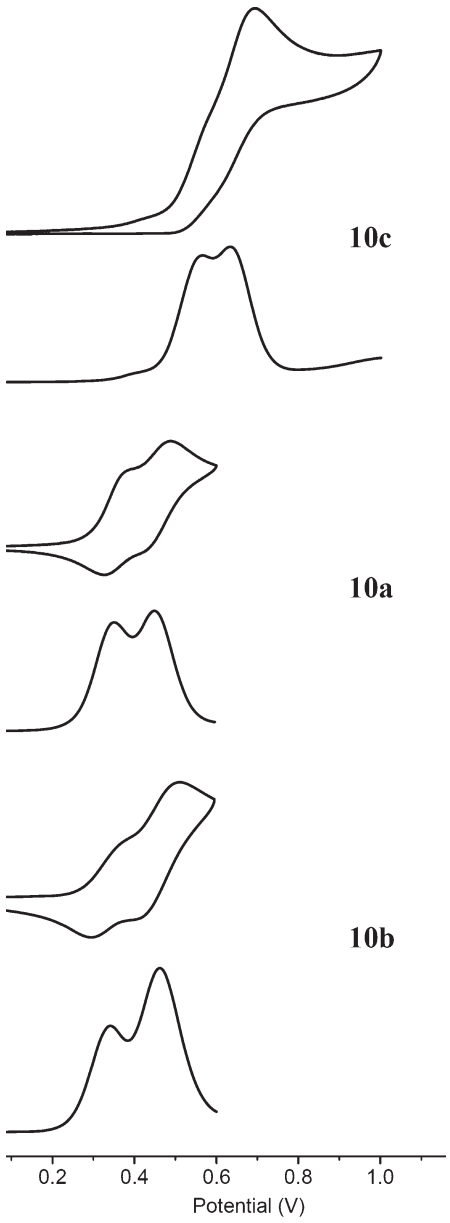

Figure 3. Cyclic voltammograms (CV) of complexes **10c**, **10a**, and **10b** in CH_2Cl_2/Bu_4NPF_6 at $v = 0.1$ V s^{-1}. Square-wave voltammograms at $f = 10$ Hz. Potentials are given relative to the $Ag|Ag^+$ standard.

to a quite large $\Delta E_{1/2}$ value of 0.12 V, as shown in Figure 3 and Table 5. Upon appending the electron-donating OC_nH_{2n+1} groups, the redox processes change from irreversible to quasi-reversible. The $\Delta E_{1/2}$ difference between complex **10b** and complex **10a** is 0.03 V, which is larger than the difference of 0.02 V between **4d** and **4a**. The above results indicate that the introduction of long carbon chains on the bridges facilitates the stability of mixed-valence complexes. We suggest that the enhanced stability of mixed-valence complexes is not entirely attributable to the electron-donating property of the OC_8H_{17} group. To some extent, the four OC_8H_{17} groups in complex **10b** are expected to act like a "coating", protecting the "bare" bridging ligand from the effects of the medium, i.e., the bulk solution, thereby preventing the loss of charge transfer.[15] That is to say, for the OC_8H_{17}-bearing structure, the enhanced stability of the mixed-valence complex is to some extent attributable to its shielding effect besides its electronic effect. Therefore, complexes such as **10b** may be viewed as potential insulated organometallic molecular wires.

The above results are supported by comparison of the voltammetric features of complexes **13a−c** in CH_2Cl_2 (Supporting Information, Figures S2 and S3 and Table S1). These three complexes all undergo one-electron oxidation processes. Upon appending the electron-donating OC_nH_{2n+1} groups, both the oxidation and reduction couples are cathodically shifted and the redox process changes from irreversible to quasi-reversible. The square-wave voltammogram (Figure S3) analyses for complexes **13a−c** show that the wave width increases following the introduction of the OC_nH_{2n+1} groups and clearly predict the presence of two unresolved (overlapping) one-electron redox couples with a $\Delta E_{1/2}$ value of approximately 80 mV for the OC_8H_{17}-bearing structure. The electrochemical properties of complexes **4a−d** and **10a**,**b** have also been investigated in THF. The results show a similar long carbon chain effect in THF to that in CH_2Cl_2 (Table S2 and Table S3).

Conclusions

We have reported here the synthesis, characterization, and electrochemical properties of a series of binuclear ruthenium vinyl complexes **4a−g** and six oligomeric binuclear ruthenium complexes (**10a−c**, **13a−c**). Electrochemical studies have shown that long carbon chains attached to the bridges of the complexes facilitate the stability of mixed-valence complexes. We suggest that the introduction of long carbon chains on the bridge causes a shielding effect besides the electronic effect.

Experimental Section

General Materials. All manipulations were carried out at room temperature under a nitrogen atmosphere using standard Schlenk techniques, unless otherwise stated. Solvent were predried, distilled, and degassed prior to use, except those for spectroscopic measurements, which were of spectroscopic grade. The starting materials $RuHCl(CO)(PPh_3)_3$,[16] **3b**,[11] **3c**,[17] **3d**,[18] **3e**,[19] **3f**,[20] and **4a**[5e] were prepared by the procedures described in literature methods. The synthesis of **2g**, **3g**, **6a−9a**, **5b−9b**, **11a**, **12a**, **11b**, and **12b** is shown in the Supporting Information.

(14) Richardson, D. E.; Taube, H. *Inorg. Chem.* **1981**, *20*, 1278.
(15) Chen, P.; Meyer, T. J. *Chem. Rev.* **1998**, *98*, 1439.
(16) Ahmad, N.; Levison, J. J.; Robinson, S. D.; Uttley, M. F.; Wonchoba, E. R.; Parshall, G. W. *Inorg. Synth.* **1974**, *15*, 45.
(17) Zhou, C.-Z.; Liu, T.; Xu, J.-M.; Chen, Z.-K. *Macromolecules* **2003**, *36*, 1457.
(18) Weder, C.; Wrighton, M. S. *Macromolecules* **1996**, *29*, 5157.
(19) Shirai, Y.; Zhao, Y.; Cheng, L.; Tour, J. M. *Org. Lett.* **2004**, *6*, 2129.
(20) Moroni, M.; Moigne, J. L.; Luzzati, S. *Macromolecules* **1994**, *27*, 562.

General Synthesis of Binuclear Ruthenium Complexes. To a suspension of $RuHCl(CO)(PPh_3)_3$ (0.76 g, 0.80 mmol) in CH_2Cl_2 (30 mL) was slowly added a solution of diethynylaryls (**4a−g**, **10a−c**, and **13a−c**) (0.50 mmol) in CH_2Cl_2 (10 mL). The reaction mixture was stirred for 30 min to give a red solution. Then a 1 M THF solution of PMe_3 (4.0 mL, 4.0 mmol) was added to the red solution. The mixture was stirred for another 15 h. The solution was filtered through a column of Celite. The volume of the filtrate was reduced to ca. 2 mL under vacuum. Addition of hexane (30 mL) to the residue produced a yellow solid, which was collected by filtration, washed with hexane, and dried under vacuum.

4b: Yield: 0.32 g, 77%. Anal. Calcd for $C_{38}H_{78}Cl_2O_4P_6Ru_2$: C, 43.14; H, 7.43. Found: C, 43.41; H, 7.53. ^{31}P NMR (160 MHz, $CDCl_3$): δ −21.10 (t, J = 21.1 Hz), −9.35 (d, J = 21.1 Hz). ^1H NMR (400 MHz, $CDCl_3$): δ 0.94 (t, J = 6.4 Hz, 6H, CH_3), 1.40 (t, J = 3.2 Hz, 36H, PMe_3), 1.47 (d, J = 6.8 Hz, 18H, PMe_3), 1.60−1.66 (m, 4H, CH_2), 1.72−1.79 (m, 4H, CH_2), 3.94 (t, J = 6.4 Hz, 4H, OCH_2), 6.93−7.00 (m, 2H, Ph−CH=), 7.04 (s, 2H, Ph−H), 7.80−7.87 (m, 2H, Ru−CH=). ^{13}C NMR (100 MHz, $CDCl_3$): δ 13.82, 16.56 (t, J = 14.8 Hz, PMe_3), 20.01 (d, J = 20.1 Hz, PMe_3), 22.40, 31.70, 69.65, 110.05, 128.24, 128.77, 149.06, 162.04, 202.18 (CO). IR (KBr, cm^{-1}): 1918 (CO), 1556, 1469, 1421 (C=C aryl, vinyl).

4c: Yellow solid, yield: 0.27 g, 48%. Anal. Calcd for $C_{42}H_{86}Cl_2O_4P_6Ru_2$: C, 45.28; H, 7.78. Found: C, 45.61; H, 8.06. ^{31}P NMR (162 MHz, $CDCl_3$): δ −22.20 (t, J = 18.1 Hz), −10.33 (d, J = 18.1 Hz). ^1H NMR (400 MHz, $CDCl_3$): δ 0.88 (t, J = 6.4 Hz, 6H CH_3), 1.23−1.31 (m, 8H, CH_2), 1.40 (t, J = 3.2 Hz, 36H, PMe_3), 1.47 (d, J = 3.2 Hz, 18H, PMe_3), 1.62−1.67 (m, 4H, CH_2), 1.73−1.80 (m, 4H, CH_2), 3.93 (t, J = 6.4 Hz, 4H, OCH_2), 6.92−7.00 (m, 2H, Ph−CH=), 7.03 (s, 2H, Ph−H), 7.80−7.87 (m, 2H, Ru−CH=). ^{13}C NMR (100 MHz, $CDCl_3$): δ 13.84, 16.31 (t, J = 15.2 Hz, PMe_3), 19.94 (d, J = 20.2 Hz, PMe_3), 22.30, 25.65, 29.54, 31.46, 69.85, 109.95, 128.10, 128.64, 148.96, 162.38, 202.06 (CO). IR (KBr, cm^{-1}): 1921 (CO), 1555, 1468, 1422 (C=C aryl, vinyl).

4d: Yellow solid, yield: 0.49 g, 84%. Anal. Calcd for $C_{46}H_{94}Cl_2O_4P_6Ru_2$: C, 47.22; H, 8.10. Found: C, 47.41; H, 8.34. ^{31}P NMR (160 MHz, $CDCl_3$): δ −19.41 (t, J = 21.1 Hz, PMe_3), −7.63 (d, J = 21.1 Hz, PMe_3). ^1H NMR (400 MHz, $CDCl_3$): δ 0.87 (t, J = 6.4 Hz, 6H, CH_3), 1.26−1.27 (m, 16H, CH_2), 1.39 (t, J = 3.2 Hz, 36H, PMe_3), 1.47 (d, J = 6.8 Hz, 18H, PMe_3), 1.51−1.52 (m, 4H, CH_2), 1.73−1.78 (m, 4H, CH_2), 3.93 (t, J = 6.4 Hz, 4H, OCH_2), 6.94−6.98 (m, 2H, Ph−CH=), 7.02 (s, 2H, Ph−H), 7.79−7.86 (m, 2H, Ru−CH=). ^{13}C NMR (100 MHz, $CDCl_3$): δ 13.88, 16.35 (t, J = 15.2 Hz, PMe_3), 19.96 (d, J = 20.5 Hz, PMe_3), 22.40, 25.99, 29.97, 29.24, 29.62, 31.55, 69.89, 109.97, 128.17, 128.70, 149.00, 162.34, 202.02 (CO). IR (KBr, cm^{-1}): 1924 (CO), 1550, 1467, 1422 (C=C aryl, vinyl).

4e: Yellow solid, yield: 0.36 g, 65%. Anal. Calcd for $C_{50}H_{102}Cl_2O_4P_6Ru_2$: C, 48.97; H, 8.38. Found: C, 48.63; H, 8.16. ^{31}P NMR (160 MHz, $CDCl_3$): δ −19.04 (t, J = 21.1 Hz, PMe_3), −7.24 (d, J = 21.1 Hz, PMe_3). ^1H NMR (400 MHz, $CDCl_3$): δ 0.88 (t, J = 6.4 Hz, 6H, CH_3), 1.26−1.27 (m, 24H, CH_2), 1.39 (t, J = 3.2 Hz, 36H, PMe_3), 1.47 (d, J = 6.4 Hz, 18H, PMe_3), 1.57−1.59 (m, 4H, CH_2), 1.76−1.77 (m, 4H, CH_2), 3.92 (t, J = 6.4 Hz, 4H, OCH_2), 6.93−6.97 (m, 2H, Ph−CH=), 7.02 (s, 2H, Ph−H), 7.79−7.82 (m, 2H, Ru−CH=). ^{13}C NMR (100 MHz, $CDCl_3$): δ 13.90, 16.34 (t, J = 15.2 Hz, PMe_3), 19.95 (d, J = 20.5 Hz, PMe_3), 22.39, 25.99, 29.06, 29.28, 29.62, 31.61, 69.88, 109.95, 128.16, 128.70, 148.99, 161.96, 202.00 (CO). IR (KBr, cm^{-1}): 1926 (CO), 1550, 1467, 1423 (C=C aryl, vinyl).

4f: Yellow solid, yield: 0.28 g, 54%. Anal. Calcd for $C_{54}H_{110}Cl_2O_4P_6Ru_2$: C, 50.58; H, 8.65. Found: C, 50.39; H, 8.93. ^{31}P NMR (160 MHz, $CDCl_3$): δ −20.52 (t, J = 21.1 Hz, PMe_3), −8.67 (d, J = 21.1 Hz, PMe_3). ^1H NMR (400 MHz, $CDCl_3$): δ 0.88 (t, J = 6.4 Hz, 6H, CH_3), 1.25−1.26 (m, 32H, CH_2), 1.40 (t, J = 3.2 Hz, 36H, PMe_3), 1.47 (d, J = 6.4 Hz, 18H, PMe_3), 1.67−1.69 (m, 4H, CH_2), 1.73−1.78 (m, 4H, CH_2), 3.92 (t, J = 6.4 Hz, 4H, OCH_2), 6.92−6.98 (m, 2H, Ph−CH=), 7.02 (s, 2H, Ph−H), 7.79−7.86 (m, 2H, Ru−CH=). ^{13}C NMR (100 MHz, $CDCl_3$): δ 13.92, 16.37 (t, J = 14.8 Hz, PMe_3), 19.98 (d, J = 20.5 Hz, PMe_3), 22.42, 26.02, 29.11, 29.36, 29.65, 31.67, 69.89, 10.97, 128.16, 128.73, 149.01, 161.56, 202.09 (CO). IR (KBr, cm^{-1}): 1925 (CO), 1550, 1467, 1422 (C=C aryl, vinyl).

4g: Yellow solid, yield: 0.49 g, 73%. Anal. Calcd for $C_{58}H_{118}Cl_2O_4P_6Ru_2$: C, 52.05; H, 8.89. Found: C, 52.31; H, 9.10. ^{31}P NMR (160 MHz, $CDCl_3$): δ −19.41 (t, J = 21.1 Hz, PMe_3), −7.64 (d, J = 21.1 Hz, PMe_3). ^1H NMR (400 MHz, $CDCl_3$): δ 0.88 (t, J = 6.4 Hz, 6H, CH_3), 1.23−1.25 (m, 40H, CH_2), 1.39 (t, J = 3.2 Hz, 36H, PMe_3), 1.47 (d, J = 6.8 Hz, 18H, PMe_3), 1.63−1.68 (m, 4H, CH_2), 1.73−1.80 (m, 4H, CH_2), 3.92 (t, J = 6.4 Hz, 4H, OCH_2), 6.92−7.00 (m, 2H, Ph−CH=), 7.02 (s, 2H, Ph−H), 7.78−7.86 (m, 2H, Ru−CH=). ^{13}C NMR (100 MHz, $CDCl_3$): δ 13.88, 16.31 (t, J = 15.3 Hz, PMe_3), 19.93 (d, J = 20.1 Hz, PMe_3), 22.39, 25.99, 29.0, 29.40, 31.63, 69.81, 109.89, 128.13, 128.72, 148.97, 201.90 (CO). IR (KBr, cm^{-1}): 1926 (CO), 1550, 1469, 1423 (C=C aryl, vinyl).

10a: Yellow solid, 0.42 g, 82%. Anal. Calcd for $C_{42}H_{74}Cl_2O_6P_6Ru_2$: C, 44.49; H, 6.58. Found: C, 44.65; H, 6.83. ^{31}P NMR (160 MHz, $CDCl_3$): δ −20.68 (t, J = 22.5 Hz, PMe_3), −8.73 (d, J = 22.5 Hz, PMe_3). ^1H NMR (600 MHz, $CDCl_3$): δ 1.40 (t, J = 3.6 Hz, 36H, PMe_3), 1.47 (d, J = 6.6 Hz, 18H, PMe_3), 3.80 (s, 6H, OCH_3), 3.91 (s, 6H, OCH_3), 6.93−6.97 (m, 2H, PH−CH=), 6.98 (s, 2H, Ph−H), 7.02 (s, 2H, Ph−H), 8.13−8.17 (m, 2H, Ru−CH=). ^{13}C NMR (100 MHz, $CDCl_3$): δ 13.90, 16.30 (t, J = 15.2 Hz, PMe_3), 19.76 (d, J = 20.9 Hz, PMe_3), 56.46, 90.09, 107.35, 108.32, 116.14, 127.87, 131.68, 148.27, 154.47, 169.10, 201.93 (CO). IR (KBr, cm^{-1}): 1918 (CO), 1561, 1533, 1485, 1464, 1420 (C=C aryl, vinyl).

10b: Yellow solid, 0.15 g, 22%. Anal. Calcd for $C_{70}H_{130}Cl_2O_6P_6Ru_2$: C, 55.07; H, 8.58. Found: C, 55.23; H, 8.61. ^{31}P NMR (160 MHz, $CDCl_3$): δ −20.48 (t, J = 22.5 Hz, PMe_3), −8.54 (d, J = 22.5 Hz, PMe_3). ^1H NMR (400 MHz, $CDCl_3$): δ 0.86 (t, J = 6.8 Hz, 12H, CH_3), 1.40 (t, J = 3.2 Hz, 36H, PMe_3), 1.25−1.26 (m, 32H, CH_2), 1.44−1.45 (m, 8H, CH_2), 1.48 (d, J = 6.8 Hz, 18H, PMe_3), 1.74−1.84 (m, 8H, CH_2), 3.90 (m, 4 Hz, OCH_2), 4.03 (m, 4 Hz, OCH_2), 6.86−6.93 (m, 2H, PhCH=), 6.97 (s, 2H, Ph−H), 7.02 (s, 2H, Ph−H), 8.04−8.12 (m, 2H, RuCH=). ^{13}C NMR (100 MHz, $CDCl_3$): δ 13.94, 16.34 (t, J = 15.2 Hz, PMe_3), 19.76 (d, J = 20.5 Hz, PMe_3), 22.48, 25.91, 26.02, 29.06, 29.15, 29.24, 29.36, 29.49, 31.62, 31.68, 66.02, 69.82, 79.78, 90.20, 109.73, 117.29, 128.34, 131.84, 147.96, 154.13, 167.82, 201.98 (CO). IR (KBr, cm^{-1}): 1922 (CO), 1561, 1533, 1493, 1467, 1419 (C=C aryl, vinyl).

10c: Yellow solid, yield: 63%. Anal. Calcd for $C_{38}H_{66}Cl_2O_2P_6Ru_2$: C, 45.02; H, 6.56. Found: C, 44.92; H, 6.82. ^{31}P NMR (160 MHz, $CDCl_3$): δ −18.96 (t, J = 22.4 Hz, PMe_3), −7.23 (d, J = 22.4 Hz, PMe_3). ^1H NMR (400 MHz, $CDCl_3$): δ 1.39 (t, J = 3.2 Hz, 36H, PMe_3), 1.48 (d, J = 6.8 Hz, 18H, PMe_3), 6.55−6.58 (m, 2H, Ph−CH=), 7.27 (d, J = 8.0 Hz, 4H, Ph−H), 7.39 (d, J = 8.0 Hz, 4H, Ph−H), 8.23−8.26 (m, 2H, Ru−CH=). ^{13}C NMR (100 MHz, $CDCl_3$): δ 16.55 (t, J = 15.2 Hz, PMe_3), 20.01 (d, J = 20.1 Hz, PMe_3), 89.73, 134.26, 118.88, 124.10, 131.51, 140.65, 168.98, 202.34 (CO). IR (KBr, ν in cm^{-1}): 1918 (CO), 1563, 1531, 1510, 1421 (C=C aryl, vinyl).

13a: Yellow solid, 0.16 g, 25%. Anal. Calcd for $C_{52}H_{82}Cl_2O_8P_6Ru_2$: C, 48.26; H, 6.39. Found: C, 48.34; H, 6.61. ^{31}P NMR (240 MHz, $CDCl_3$): δ −19.17 (t, J = 21.1 Hz, PMe_3), −7.32 (d, J = 22.1 Hz, PMe_3). ^1H NMR (600 MHz, $CDCl_3$): δ 1.41 (t, J = 3.6 Hz, 36H, PMe_3), 1.48 (d, J = 6.6 Hz, 18H, PMe_3), 3.80 (s, 2H, OCH_3), 3.91 (s, 2H, OCH_3), 3.92 (s, 2H, OCH_3), 6.94−6.95 (m, 2H, Ph−CH=), 6.97 (s, 2H, Ph−H), 7.02 (s, 2H, Ph−H), 7.04 (s, 2H, Ph−H), 8.12−8.23 (m, 2H, Ru−CH=). IR (KBr, cm^{-1}): 1918 (CO), 1561, 1533, 1505, 1487, 1464 (C=C aryl, vinyl).

13b: Yellow solid, 0.47 g, 55%. Anal. Calcd for $C_{94}H_{164}Cl_2O_8P_6Ru_2$: C, 60.02; H, 8.79. Found: C, 60.38; H, 8.59.

^{31}P NMR (160 MHz, $CDCl_3$): δ −20.43 (t, J = 22.5 Hz, PMe_3), −8.60 (d, J = 22.5 Hz, PMe_3). ^{1}H NMR (400 MHz, $CDCl_3$): δ 0.86 (t J = 6.8 Hz, 18H, CH_3), 1.26−1.27 (m, 48H, CH_2), 1.39 (t, J = 3.2 Hz, 36H, PMe_3), 1.47 (d, J = 6.8 Hz, 18H, PMe_3), 1.48−1.49 (m, 12H, CH_2), 1.72−1.86 (m, 12H, CH_2), 3.91 (t, J = 6.4, 4H, OCH_2), 4.02−4.07 (m, 8H, OCH_2), 6.94−6.95 (m, 2H, Ph−CH=), 6.99 (s, 4H, Ph−H), 7.03 (s, 4H, Ph−H), 8.12−8.17 (m, 2H, Ru−CH=). ^{13}C NMR (100 MHz, $CDCl_3$): δ 19.96, 16.39 (t, J = 15.2 Hz, PMe_3), 19.88 (d, J = 20.9 Hz, PMe_3), 22.50, 25.89, 26.04, 29.22, 29.41, 29.51, 31.73, 69.18, 69.49, 69.70, 89.27, 92.49, 108.79, 109.21, 114.25, 117.07, 117.44, 128.33, 132.48, 147.95, 153.10, 154.41, 168.97, 201.95 (CO). IR (KBr, cm^{-1}): 1925 (CO), 1555, 1526, 1506, 1467, 1423 (C=C aryl, vinyl).

13c: Yellow solid, yield: 63%. Anal. Calcd for $C_{46}H_{70}Cl_2O_2P_6Ru_2$: C, 49.60; H, 6.33. Found: C, 49.32; H, 6.58. ^{31}P NMR (240 MHz, $CDCl_3$): δ −19.04 (t, J = 21.1 Hz, PMe_3), −7.29 (d, J = 22.1 Hz, PMe_3). ^{1}H NMR (600 MHz, $CDCl_3$): δ 1.39 (t, J = 3.6 Hz, 36H, PMe_3), 1.48 (d, J = 6.6 Hz, 18H, PMe_3), 6.59−6.62 (m, 2H, Ph−CH=), 7.29 (d, J = 7.8 Hz, Ph−H), 7.42 (d, J = 7.8 Hz, Ph−H), 7.47 (d, J = 7.8 Hz, Ph−H), 8.30−8.32 (m, 2H, RuCH=). IR (KBr, cm^{-1}): 1918 (CO), 1597, 1563, 1530, 1515, 1420 (C=C aryl, vinyl).

Crystallographic Details. Crystals suitable for X-ray diffraction were grown from a dichloromethane of solution **4b** and **4d** layered with hexane. A crystal with approximate dimensions of 0.30 × 0.20 × 0.20 mm^3 for **4b** and 0.23 × 0.20 × 0.20 mm^3 for **4d** was mounted on a glass fiber for diffraction experiments. Intensity data were collected on a Nonius Kappa CCD diffractometer with Mo Kα radiation (0.71073 Å) at room temperature. The structures were solved by a combination of direct methods (SHELXS-97[22]) and Fourier difference techniques and refined by full-matrix least-squares (SHELXL-97[23]). All non-H atoms were refined anisotropically. The hydrogen atoms were placed in ideal positions and refined as riding atoms. Further crystal data and details of the data collection are summarized in Table 1. Selected bond distances and angles are given in Table 2.

Physical Measurements. ^{1}H, ^{13}C{^{1}H}, and ^{31}P{^{1}H} NMR spectra were collected on a Varian Mercury Plus 400 spectrometer (400 MHz) or on a Varian Mercury Plus 600 spectrometer (600 MHz). ^{1}H and ^{13}C{^{1}H} NMR chemical shifts are relative to TMS, and ^{31}P{^{1}H} NMR chemical shifts are relative to 85% H_3PO_4. Elemental analyses (C, H, N) were performed by Vario ElIII Chnso. IR spectra were recorded on a Nicolet Avatar 360 FT-IR spectrophotometer using KBr disks. UV−vis spectra were recorded on a PDA spectrophotometer by quartz cells with a path length of 1.0 cm. The electrochemical measurements were performed on a CHI 660C potentiostat (CHI USA). A three-electrode one-compartment cell was used to contain the solution of the compound and supporting electrolyte in dry CH_2Cl_2 and THF. Deaeration of the solution was achieved by argon bubbling through the solution for about 10 min before measurement. The ligand and electrolyte (Bu_4NPF_6) concentrations were typically 0.001 and 0.1 mol dm^{-3}, respectively. A 500 μm diameter platinum disk working electrode, a platinum wire counter electrode, and an Ag|Ag$^+$ reference electrode were used. The Ag|Ag$^+$ reference electrode contained an internal solution of 0.01 mol dm^{-3} $AgNO_3$ in acetonitrile and was incorporated to the cell with a salt bridge containing 0.1 mol dm^{-3} Bu_4NPF_6 in CH_2Cl_2. All electrochemical experiments were carried out under ambient conditions.

Supporting Information Available: The synthesis of **2g**, **3g**, **6a**−**9a**, **5b**−**9b**, **11a**, **12a**, **11b**, and **12b**, tables of bond distances and angles, and X-ray crystallographic files (CIF) for complexes **4b** and **4d**, and CVs of complexes **4b**, **4c**, **4g**, and **13a**−**c**. The materials are available free of charge via the Internet at http://pubs.acs.org.

Acknowledgment. The authors acknowledge financial support from National Natural Science Foundation of China (Nos. 20772039, 20931006) and the Natural Science Foundation of Hubei Province (No. 2008CDB023).

(21) Swager, T. M.; Gil, C. J.; Wrighton, M. S. *J. Phys. Chem.* **1995**, *99*, 4886.
(22) Sheldrick, G. M. *SHELXS-97, a program for crystal structure solution*; Göttingen, Germany, 1997.
(23) Sheldrick, G. M. *SHELXL-97, a program for crystal structure refinement*; Göttingen, Germany, 1997.